Redox change in sedimentary environments of Triassic bedded cherts, central Japan: possible reflection of sea-level change

KENICHIRO SUGITANI* & KOICHI MIMURA†

* Department of Natural Science Informatics, Nagoya University, Nagoya 464-8601, Japan
† Department of Earth and Planetary Sciences, Nagoya University, Nagoya 464-8601, Japan

(*Received* 20 August 1997; *accepted* 26 June 1998)

Abstract – Middle Triassic radiolarian bedded cherts in the Mino Belt, central Japan, include a sequence showing an abrupt facies change from the lower to the upper, where grey–black bedded cherts enriched in carbonaceous matter and framboidal pyrite are overlain by brick-red hematitic bedded cherts. Brownish-yellow chert enriched in goethite and purple-red chert occur at the boundary between the grey–black bedded cherts and the brick-red bedded cherts. This facies change is in accordance with stratigraphic variations of geochemical characteristics; the lower section grey–black bedded cherts, compared with the upper section brick-red bedded cherts, are enriched in C_{tot} and S_{tot}, and are characterized by lower MnO/TiO_2, higher FeO/Fe_2O_3* (total iron as Fe_2O_3) and more variable Fe_2O_3*/TiO_2 values. Some of the lower section samples, in addition, are characterized by an enrichment in some transition metals (Ni, Cu, and Zn). The covariation of mineralogical and geochemical characteristics indicates that sedimentary environments and diagenetic processes were different between the lower and the upper section bedded cherts. During the deposition of the lower section bedded cherts, the sedimentary environment was anoxic and bacterial sulphate reduction occurred during the early diagenetic stage. In contrast, the upper section bedded cherts were subjected to less reducing diagenetic processes; active sulphate reduction did not occur. The change of sedimentary environment and diagenetic process at the site of deposition is likely to be attributed to the fluctuated concentration of dissolved oxygen in the water mass of a semi-closed marginal ocean basin, which was potentially caused by sea-level change that occurred during Middle Triassic time.

1. Introduction

Cherts are volumetrically minor but widespread in Palaeozoic and Mesozoic orogenic belts in the world, and their origins and depositional environments have long been controversial. Various origins for cherts have been proposed: silicification of tuffaceous sediments, evaporites and carbonates, biogenic accumulation of silica (e.g., radiolarian ooze), and precipitation of hydrothermally-derived silica (e.g. Knauth, 1994; Adachi, Yamamoto & Sugisaki, 1986; Yamamoto, 1984, 1987). Detailed mineralogical and sedimentological studies of bedded cherts have not always been successful, because they consist mostly of microcrystalline quartz with minor authigenic minerals and very fine-grained detrital material. Many authors (e.g. Matsumoto & Iijima, 1983; Murray *et al.* 1991; Shimizu & Masuda, 1977; Steinberg, Bonnot-Courtis & Tlig, 1983; Sugisaki, Yamamoto & Adachi, 1982; Yamamoto, 1983) have taken geochemical approaches toward the origins and depositional environments of cherts.

Concentrations of some transition metals such as Fe and Mn in marine sediments are different between hemipelagic, pelagic and hydrothermal (near ridge) sediments; in general, their concentrations gradually decrease from near mid-ocean ridges to land (hydrothermal (near ridge) > pelagic > hemipelagic) (e.g. Sugisaki, 1984; Boström, Kraemer & Gartner, 1973). Therefore, origins and sedimentary environments of cherts can be examined by comparing chemical compositions of cherts with those of marine sediments from various depositional settings and origins (Sugitani *et al.* 1991; Sugisaki, Yamamoto & Adachi, 1982; Yamamoto, 1983; Murray, 1994; Adachi, Yamamoto & Sugisaki, 1986; Girty *et al.* 1996). However, diagenetic remobilization of these elements such as fractionation between cherts and shale-partings of bedded cherts, which evidently constrains the availability of geochemical indicators (e.g. Murray, 1994), has not always been sufficiently discussed.

In this study, we discuss the geochemical characteristics of Triassic radiolarian bedded cherts in the Mino Belt, central Japan. The bedded chert sequence shows an abrupt facies change from the lower part to the upper; grey–black bedded cherts enriched in carbonaceous matter and pyrite are overlain by purple-red and brick-red hematitic bedded cherts (Isozaki, 1997; Nakao & Isozaki, 1994; Kubo, Isozaki & Matsuo, 1996). The facies change is expected to be closely related to the fluctuation of sedimentary environment and diagenetic process. The subjects addressed here are (1) revealing stratigraphic variations of organic,

*Author for correspondence: sugi@info.human.nagoya-u.ac.jp

authigenic and clastic components in the bedded cherts and (2) appraisal of factors controlling deposition and preservation of carbonaceous matter in the bedded cherts. The detailed geochemical examinations of the bedded cherts, combined with our recent knowledge of palaeoceanography and ocean chemistry, could provide us with important information about the sedimentary environments and origins of Triassic bedded chert in the Mino Belt, central Japan.

2. Geological background, stratigraphy and sampling

The Mino Belt, one of the major geological units in southwest–central Japan, consists of chaotically mixed Permian to Triassic bedded cherts, limestones, basalts, and Jurassic turbidite sandstones and shales (Wakita, 1988) (Fig. 1). To the north of the Mino Belt, a geological unit containing Precambrian quartzo-feldspathic gneisses and schists is present (Hida Belt; Fig. 1) and is interpreted as originating from Precambrian continental fragments formerly attached to the Asian continent before the opening of the Sea of Japan. Sources for Jurassic terrigenous sediments (turbidite sandstones and shales) in the Mino Belt are derived at least partially from these older rocks (Adachi, 1976).

The Palaeozoic–Mesozoic geological history of central–southwest Japan is often interpreted by the processes of steady-state accretion of oceanic crusts and microcontinents and subduction-related igneous activities (e.g. Taira *et al.* 1992; Maruyama & Seno, 1986). The Mino Belt is generally thought to be a representative of an accretional prism (mélange) formed at ancient subduction zone (Matsuda & Isozaki, 1991). Bedded cherts in the Mino Belt occurring as blocks or lenses of various sizes within the 'matrix' turbidite sequences are thought to have been deposited in pelagic regions far from continents and accreted at an ancient subduction zone (along the Asian continental margin) (Matsuda & Isozaki, 1991). However, Cluzel (1991) claimed that the continental rifting and the extensional opening of a small oceanic basin and subsequent back-collision of the detached continental block were major orogenic processes for central–southwest Japan from the Middle Carboniferous to the Triassic. Adachi (1976) and Suzuki, Adachi & Tanaka (1991) suggested the previous presence of Precambrian continents or continental fragments on the basis of palaeocurrent data and geochronological data for Jurassic turbidite sequences. They also showed that to the south of the Mino Belt, continents or continental blocks geochronologically similar to the rocks of the Hida Belt were exposed, and implied that the site of deposition of the Mino Belt was an east–west trending elongated basin where two major detrital sources were exposed to the north and the south of the basin.

We collected bedded chert samples (cherts and their shale-partings) at an outcrop along the Kiso River, Kagamigahara City, Gifu Prefecture (Fig. 1), where

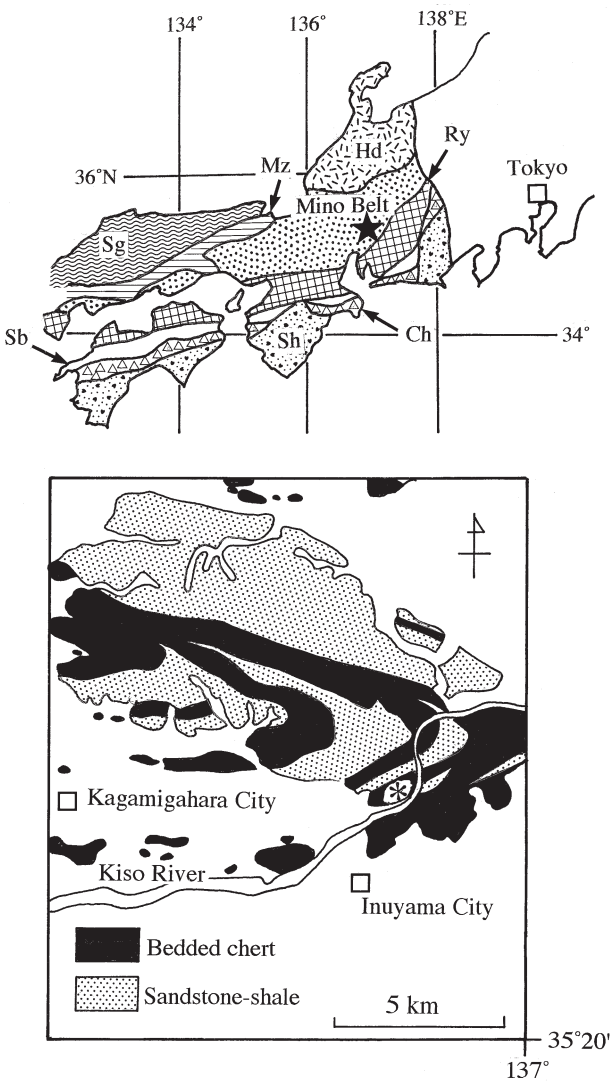

Figure 1. Tectonic divisions of central–southwest Japan (after Mizutani, 1987) and local geological map of our sampling site (after Geological Survey of Japan, 1992). Hd: Hida Belt, Mz: Maizuru Belt; Sg: Sangun Belt; Sb: Sambagawa Belt; Ry: Ryoke Belt; Sh: Shimanto Belt; Ch: Chichibu Belt. The star in the tectonic division map shows the area of our sampling site. The asterisk in the local geological map shows the sampling site along the Kiso River.

three Triassic chert units (CH1, CH2, CH3; Yao, Matsuda & Isozaki, 1980) occur as large blocks within Jurassic turbidite sequences. At the sampling site (the asterisk in the local geological map of Fig. 1), the bedded chert sequence (CH2) is well stratified and five colour types of cherts are recognized by Nakao & Isozaki (1994), who subdivided the sequence into four units: from the base upwards, grey–black bedded cherts, brownish-yellow chert, purple-red chert, and brick-red bedded cherts occur (Fig. 2). The brownish-yellow chert and purple-red chert lack shale-partings, whereas the grey–black bedded cherts and brick-red cherts consist of an alternation of chert beds and shale-partings up to several centimetres thick. Shale-partings within the bedded chert at the sampling site are generally thicker than

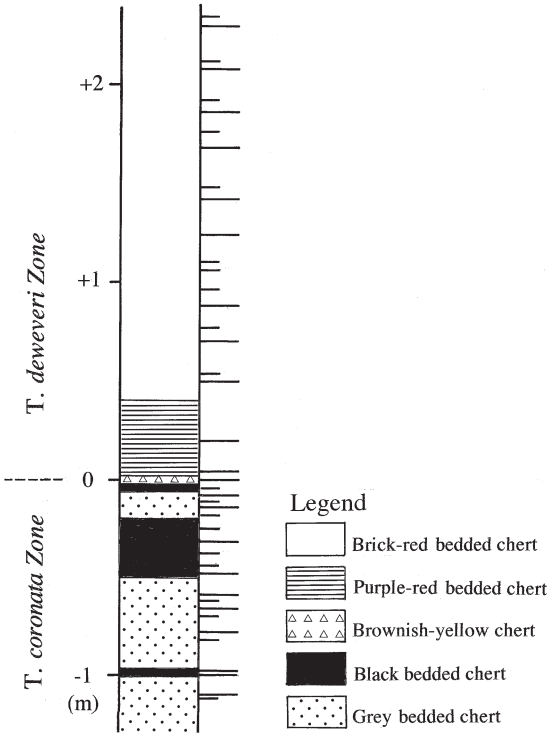

Figure 2. Stratigraphic column of the bedded chert sequence. The long and short lateral bars indicate the sampling positions of cherts and shale-partings, respectively. We designate the brownish-yellow cherts as a boundary key bed (0 m) between the lower grey–black bedded cherts and the upper brick-red and purple-red bedded cherts. Radiolarian zonation is after Sugiyama (1995).

those in typical Triassic bedded chert found in the Mino Belt (< 1 cm). Middle Triassic (Anisian) radiolaria were extracted from this bedded chert sequence, and the brownish-yellow chert approximately corresponds to the biostratigraphic boundary between the *T. coronata* Zone and *T. deweveri* Zone (Sugiyama, 1995).

3. Petrological characteristics

Optically identifiable components in the bedded cherts are carbonaceous matter, framboidal and euhedral pyrite, tests of siliceous organisms (mostly radiolaria), authigenic quartz (chalcedony and microcrystalline quartz), fine silicate minerals, red clay (very fine red–brown material; Nisbet & Price, 1974) and yellowish clay. Nakao & Isozaki (1994) and Kubo, Isozaki & Matsuo (1996) showed the presence of hematite (probably the major constituent of the red clay) by X-ray diffractometry and ^{57}Fe Mössbauer analyses. The yellowish clay characteristically present in the brownish-yellow chert is very fine material and its individual grains cannot be optically identifiable; ^{57}Fe Mössbauer analysis operated by Kubo, Isozaki & Matsuo (1996) shows that the yellowish clay is composed of goethite. Abundances of these components are quite different between types of chert and detailed descriptions are given below.

3.a. Grey–black bedded chert

The grey–black bedded cherts, especially black bedded cherts, are characterized by abundant carbonaceous matter and pyrite, and do not contain hematite (Nakao & Isozaki, 1994; Kubo, Isozaki & Matsuo, 1996). Other constituents are microcrystalline quartz, radiolarian tests and fine silicate minerals. Carbonaceous matter in the grey–black bedded cherts is generally structureless and fine-grained, but in some portions shows microbial structures. Minute spheroids (< 5 μm) thinly-walled with carbonaceous matter are common, and large spheroids (~20 μm) containing carbonaceous spherules are rarely found (Fig. 3a). These carbonaceous spheroids are possible relicts of micro-organisms. Pyrite in the grey–black bedded chert occurs as euhedral grains or framboids. Euhedral pyrite grains are generally present inside radiolarian tests that have been filled with fibrous microcrystalline quartz, whereas framboidal pyrite generally occurs in the matrix which is composed of microcrystalline quartz and other impurities (Fig. 3b).

3.b. Brownish-yellow chert

The brownish-yellow chert consists of alternations of partly brecciated yellow layers and bright-red layers a few millimetres thick. The chert contains thin layers composed of chalcedony, where fibrous quartz crystals grow both from the upper layer and the lower one (Fig. 3c). The red layer is enriched in red clay, whereas the brownish-yellow layer contains yellowish clay (goethite) (Kubo, Isozaki & Matsuo, 1996). Radiolarian tests are not abundant in portions where red clay or yellowish clay is densely distributed. Carbonaceous matter and pyrite are not found.

3.c. Purple-red cherts and brick-red bedded cherts

The purple-red chert and brick-red bedded cherts are petrologically similar with each other; they are free from pyrite, carbonaceous matter, and goethite. Both the cherts commonly contain hematite (Kubo, Isozaki & Matsuo, 1996; Nakao & Isozaki, 1994). Hematite in the purple-red cherts occurs as fine but microscopically identifiable particles, whereas individual hematite particles in the brick-red bedded cherts cannot be identified under the microscope. The lowermost two brick-red cherts (St. 1–24, 26) contain authigenic carbonate grains (Fig. 3d).

4. Analytical methods

Major and minor elements were analysed by an X-ray fluorescence spectrometer (XRF). For major elements, a fusion glass made from the mixture of powdered sample and flux ($Li_2B_4O_7$) in the proportion of 1 : 5 was used (Sugisaki, Shimomura & Ando, 1977). For

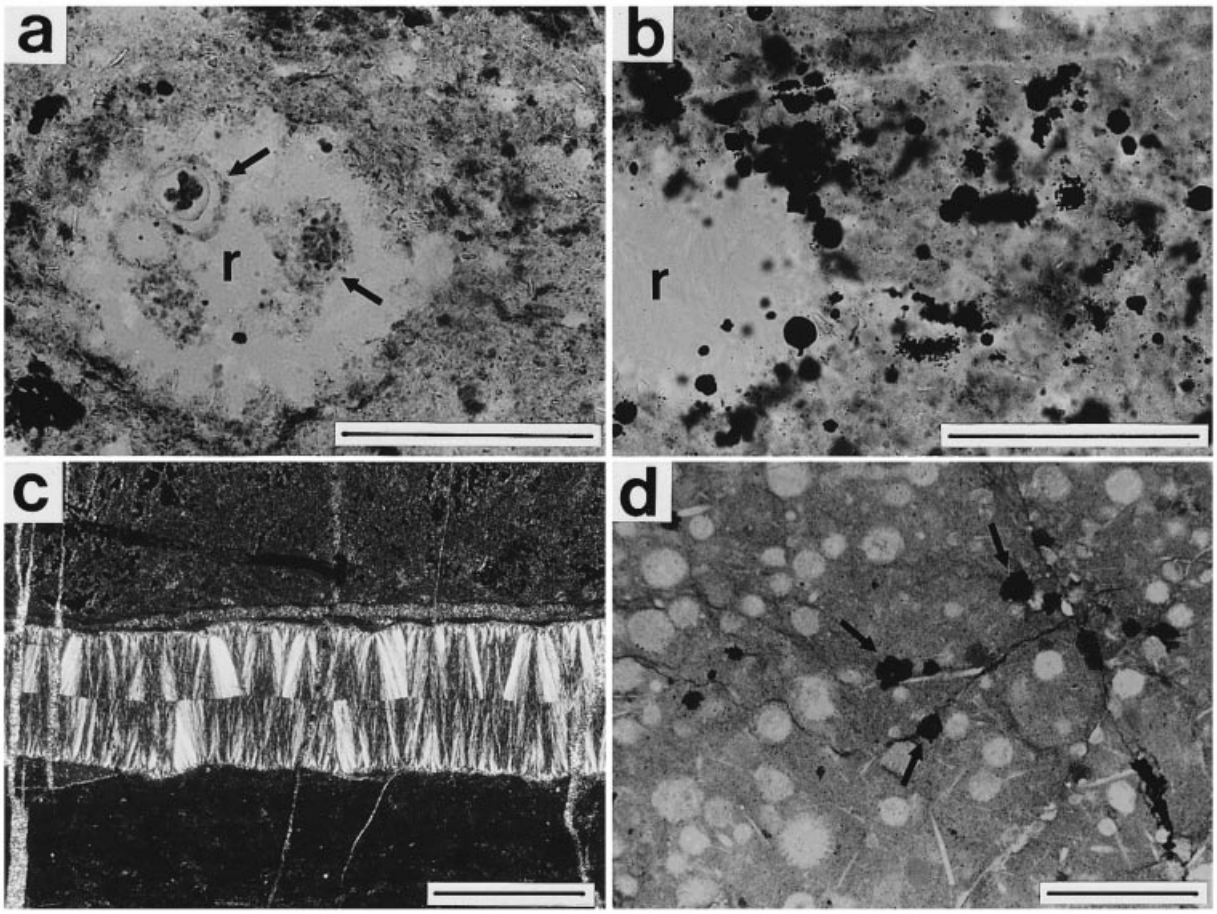

Figure 3. Photomicrographs of bedded chert samples. (a) Microbial textures composed of carbonaceous materials (arrows) inside the radiolarian test (r). Scale bar is 100 μm. (b) Framboidal pyrite (black) in the matrix of the black chert; r shows a radiolarian test. Scale bar is 100 μm. (c) Quartz vein composed of chalcedony in the brownish-yellow chert. Scale bar is 500 μm. (d) Brick-red bedded chert containing authigenic carbonates (arrowed; probably $MnCO_3$). Scale bar is 500 μm.

minor elements, a pressed disc made from the mixture of powdered sample and binder in the proportion of 2 : 3 was used. Total C, H (recalculated to H_2O), and S were analysed by an elemental analyser (Fisons EA1108). Ferrous iron was determined by the colourimetric method using *o*-phenanthroline after decomposition of the samples by HF-H_2SO_4 (Sugisaki, 1981). Pyrite (FeS_2) cannot completely be decomposed during this procedure (Sugisaki, 1981), and therefore FeO concentrations determined by this method show the fraction of FeO in labile phases (e.g. silicates) and a part of pyrite. The analytical results, and analytical precision and accuracy for XRF analyses are listed in Tables 1 and 2, respectively.

5. Result and discussion

5.a. Carbon and sulphur

The most conspicuous geochemical features of the bedded cherts are high concentrations of C_{tot} (~4.19%) and S_{tot} (~3.88%) in the lower section samples (grey–black bedded cherts) (Table 1). Concentrations of C_{tot} and S_{tot} in the upper section samples (purple-red chert and brick-red bedded cherts) are mostly less than 0.02% and less than the detection limit (0.01%), respectively (Fig. 4). The high concentrations of C_{tot} and S_{tot} in the lower sections are mainly attributed to carbonaceous matter and pyrite.

It is generally accepted that authigenic pyrite (framboidal pyrite) is formed within the sulphate reduction zone of a sedimentary column during early diagenesis (e.g. Berner, 1984); bacterial sulphate reduction under anoxic environments produces H_2S that reacts with dissolved Fe^{2+} to form authigenic pyrite. Thus, the presence of framboidal pyrite associated with carbonaceous matter (including relicts of micro-organisms) in the grey–black bedded cherts shows that bacterial sulphate reduction occurred during early diagenesis. In contrast, the purple-red chert and brick-red bedded cherts without microscopically identifiable carbonaceous matter and pyrite were subjected to less reducing diagenetic processes. The different diagenetic processes between the lower and upper sections will be discussed in detail later (Section 6.a).

Table 1. Chemical compositions of cherts and shales

Sample No.	St.1–1	St.1–2	St.1–3	St.1–4	St.1–5	St.1–6	St.1–7	St.1–8	St.1–9	St.1–10	St.1–11	St.1–12	St.1–13	St.1–14
colour-type	gr	gr	blk	blk	gr	gr	gr	gr	gr	gr	blk	blk–gr	blk	blk
SiO_2(wt%)	79.29	92.01	89.39	88.68	68.20	93.97	70.15	93.27	71.47	90.93	93.91	67.98	94.16	58.95
TiO_2	0.44	0.14	0.12	0.12	0.69	0.11	0.61	0.11	0.58	0.15	0.099	0.69	0.078	0.76
Al_2O_3	8.94	3.17	2.09	2.27	14.29	2.31	13.24	2.35	12.28	3.14	2.19	14.26	1.54	15.03
Fe_2O_3(total)	3.81	1.16	1.13	1.05	4.48	0.83	4.04	1.15	4.40	1.37	0.88	4.14	0.76	10.00
MnO	0.019	0.009	0.003	0.004	0.067	0.015	0.041	0.020	0.036	0.016	0.018	0.045	0.014	0.081
MgO	1.08	0.39	0.18	0.23	2.35	0.38	2.24	0.47	2.03	0.53	0.39	2.27	0.22	2.24
CaO (total)	0.02	0.04	0.01	0.03	0.12	0.08	0.06	0.06	0.04	0.07	0.05	0.02	0.06	0.06
Na_2O	0.05	0.09	<0.05	<0.05	<0.05	<0.05	<0.05	0.06	<0.05	<0.05	<0.05	<0.05	<0.05	<0.05
K_2O	2.49	0.85	0.63	0.69	4.24	0.62	4.01	0.60	3.75	0.91	0.54	4.16	0.39	4.52
P_2O_5	0.07	0.02	0.01	0.02	0.08	0.03	0.07	0.02	0.07	0.03	0.02	0.07	0.03	0.10
H_2O*	2.89	0.97	2.24	2.60	4.29	0.98	3.95	0.96	3.90	1.10	0.88	4.62	0.81	5.17
C**	0.05	0.02	4.08	4.19	0.07	0.01	0.05	0.01	0.08	0.01	0.03	0.35	0.20	2.23
S***	0.14	0.32	0.31	0.34	0.02	0.08	0.08	0.19	0.71	0.32	0.17	0.50	0.25	3.88
FeO#	0.39	0.14	0.27	0.32	1.17	0.21	1.20	0.27	0.89	0.33	0.21	1.01	0.08	1.44
total	99.29	99.19	100.19	100.22	98.90	99.42	98.54	99.27	99.35	98.58	99.18	99.11	98.51	103.02
Cr(ppm)	40	20	80	100	60	<10	60	20	60	30	<10	70	<10	120
Co	<10	<10	10	30	<10	<10	10	<10	<10	<10	<10	10	10	70
Ni	10	20	120	160	40	20	40	20	40	30	30	90	50	380
Cu	50	40	40	70	80	20	80	20	80	30	40	380	50	310
Zn	50	40	30	30	80	30	80	20	100	30	40	240	50	190
Rb	100	40	30	30	160	20	160	20	150	40	20	160	10	130
Sr	50	30	20	20	40	30	40	30	40	30	30	40	20	40
Y	20	<10	10	<10	30	10	20	<10	20	10	<10	30	<10	40
Zr	80	30	40	40	130	20	120	20	120	30	20	130	20	160
Pb	10	,10	<10	<10	20	<10	10	<10	20	<10	<10	20	<10	40
Ba	250	150	100	100	350	100	350	100	350	150	100	350	100	350

Table 1 (*cont.*)

Sample No.	St.1–15	St.1–16	St.1–17	St.1–18	St.1–19	St.1–20	St.1–21	St.1–22	St.1–23	St.1–24	St.1–25	St.1–26	St.1–27	St.1–28
colour-type	blk	blk–gr	gr	blk–gr	gr	blk	by	rp	rp	br	br	br	br	br
SiO_2(wt%)	96.23	78.19	93.66	71.12	92.60	73.05	92.76	87.66	93.07	89.00	69.83	91.40	68.20	89.93
TiO_2	0.089	0.41	0.13	0.58	0.12	0.46	0.10	0.21	0.10	0.19	0.55	0.14	0.61	0.16
Al_2O_3	1.78	9.05	2.64	12.41	2.66	9.86	1.95	3.98	2.12	3.85	11.77	2.82	13.07	3.28
Fe_2O_3(total)	0.75	4.13	0.95	4.93	1.23	4.17	2.08	2.61	0.93	2.67	6.46	1.43	6.25	1.57
MnO	0.010	0.057	0.010	0.036	0.012	0.021	0.014	0.025	0.009	0.14	0.080	0.15	0.20	0.049
MgO	0.24	1.82	0.39	2.05	0.52	1.47	0.35	0.75	0.32	0.75	2.23	0.50	2.49	0.62
CaO (total)	0.05	0.08	0.05	0.11	0.05	0.08	0.07	0.12	0.08	0.13	0.21	0.09	0.28	0.10
Na_2O	<0.05	<0.05	<0.05	0.05	<0.05	0.05	<0.05	<0.05	<0.05	0.06	<0.05	<0.05	<0.05	0.09
K_2O	0.42	2.29	0.72	3.73	0.65	2.89	0.57	1.30	0.65	1.15	3.79	0.82	4.27	1.05
P_2O_5	0.02	0.08	0.02	0.07	0.02	0.07	0.03	0.05	0.03	0.06	0.10	0.03	0.15	0.04
H_2O*	0.83	2.77	0.94	4.03	1.16	4.49	0.81	1.44	0.81	1.35	3.87	0.63	4.14	1.08
C**	0.22	0.38	0.01	0.07	0.05	3.92	<0.01	<0.01	0.01	<0.01	0.03	0.10	0.03	0.03
S***	0.23	0.45	0.07	0.31	0.01	0.49	<0.01	0.04	<0.01	<0.01	<0.01	0.02	<0.01	<0.01
FeO#	0.13	1.58	0.42	2.40	0.48	0.92	0.53	0.68	0.28	0.35	0.77	0.21	0.55	0.23
total	100.87	99.71	99.59	99.50	99.19	101.02	98.73	98.19	98.13	99.35	98.92	98.13	99.69	98.00
Cr(ppm)	20	80	<10	70	<10	160	40	50	<10	10	40	20	60	20
Co	20	40	10	20	<10	100	<10	<10	<10	<10	10	<10	20	<10
Ni	50	80	20	70	20	180	20	20	10	20	50	20	60	20
Cu	400	170	100	150	30	730	20	20	20	50	70	60	70	70
Zn	130	120	20	80	40	120	40	70	30	50	140	30	140	40
Rb	10	80	30	140	30	110	30	60	30	50	150	40	170	50
Sr	30	40	30	50	30	40	30	40	30	40	40	40	40	40
Y	20	20	<10	30	<10	30	10	10	<10	20	30	<10	30	<10
Zr	20	90	30	110	30	100	20	50	20	40	110	30	120	30
Pb	10	20	10	20	<10	100	<10	<10	<10	20	20	<10	20	<10
Ba	100	250	100	300	100	250	100	200	100	150	400	150	450	150

Sample No.	St.1–29	St.1–30	St.1–131	St.1–32	St.1–33	St.1–34	St.1–35	St.1–36	St.1–37	St.1–38	St.1–39	St.1–40	St.1–41	St.1–42
colour-type	br	br	br	br	br	br	br	br	br	br	br	br	br	br
SiO_2(wt%)	74.67	82.93	70.10	91.31	89.45	71.87	91.39	69.49	88.28	68.39	90.45	70.83	90.78	71.04
TiO_2	0.47	0.33	0.58	0.16	0.19	0.54	0.14	0.58	0.21	0.57	0.16	0.56	0.16	0.53
Al_2O_3	9.95	6.47	12.50	3.16	3.76	11.39	2.91	12.28	4.04	12.43	3.20	11.71	3.28	11.28
Fe_2O_3(total)	4.49	3.09	5.63	1.46	1.85	5.41	1.44	5.60	2.04	5.65	1.55	5.35	1.57	5.02
MnO	0.23	0.079	0.20	0.032	0.038	0.094	0.053	0.16	0.050	0.15	0.040	0.10	0.038	0.13
MgO	1.81	1.19	2.45	0.55	0.82	2.24	0.81	2.62	0.77	2.53	0.63	2.14	0.58	2.00
CaO (total)	0.27	0.16	0.39	0.25	0.14	0.49	0.10	0.65	0.15	0.91	0.19	0.70	0.11	1.14
Na_2O	0.12	0.07	0.06	<0.05	<0.05	0.07	<0.05	0.12	<0.05	<0.05	<0.05	0.13	<0.05	0.11
K_2O	3.18	2.01	4.01	0.99	1.06	3.62	0.84	3.89	1.41	3.98	0.98	3.87	1.02	3.77
P_2O_5	0.08	0.07	0.21	0.14	0.06	0.29	0.04	0.37	0.06	0.54	0.09	0.44	0.05	0.69
H_2O*	3.33	2.16	3.78	1.08	1.35	3.69	1.26	4.41	1.53	4.23	1.17	4.14	1.26	3.78
C**	0.03	0.01	0.01	0.01	0.01	0.02	0.01	0.02	0.01	0.02	<0.01	0.03	0.01	0.02
S***	<0.01	<0.01	<0.01	<0.01	<0.01	<0.01	<0.01	<0.01	<0.01	<0.01	<0.01	<0.01	<0.01	<0.01
FeO#	0.38	0.33	0.65	0.22	0.28	0.65	0.23	0.86	0.18	0.86	0.12	0.66	0.15	0.42
total	98.63	98.57	99.92	99.14	98.73	99.72	98.99	100.19	98.55	99.40	98.46	100.00	98.86	99.51
Cr(ppm)	30	30	50	30	20	40	<10	40	<10	40	20	40	<10	30
Co	20	10	20	<10	<10	20	<10	20	<10	20	10	10	<10	10
Ni	50	30	60	20	20	60	20	70	20	70	20	60	20	60
Cu	80	60	60	70	50	40	60	60	70	60	60	50	80	40
Zn	110	70	120	40	50	130	50	140	50	140	40	130	40	120
Rb	130	90	160	50	50	150	40	150	60	160	40	150	50	150
Sr	40	40	40	40	40	40	30	40	40	40	40	40	40	50
Y	20	20	20	10	10	30	<10	30	10	30	10	30	<10	30
Zr	90	60	110	30	40	110	30	110	40	110	30	110	30	100
Pb	10	<10	20	<10	<10	10	10	20	<10	10	<10	20	<10	10
Ba	350	300	350	150	150	350	150	350	150	400	150	350	150	400

gr = grey; blk = black; rp = reddish purple; br = brick-red; by = brownish-yellow.
*Total H is recalculated as H_2O.
**Total C; ***total S; # FeO in fraction decomposed by HF–H_2SO_4.

Table 2. Precisions and accuracies of XRF analyses

	JG1(n=6)	
	av. (sd)	r.v.
SiO_2(wt%)	72.35 (0.77)	72.28
TiO_2	0.30 (0.02)	0.27
Al_2O_3	14.48 (0.10)	14.23
Fe_2O_3(total)	2.16 (0.01)	2.17
MnO	0.067 (0.012)	0.061
MgO	0.75 (0.06)	0.73
CaO	2.24 (0.02)	2.17
Na_2O	3.71 (0.17)	3.38
K_2O	3.95 (0.02)	3.96
P_2O_5	0.10 (0.004)	0.10

	G2(n=5)		Jch–1(n=5)	
	av. (sd)	r.v.	av. (sd)	r.v.
Cr(ppm)	1 (2)	9	25 (3)	9
Co	7 (1)	6	20 (2)	15
Ni	8 (1)	6	17 (1)	7.5
Cu	12 (1)	11	23 (1)	15.5
Zn	83 (1)	85	12 (1)	9.1
Rb	171 (1)	170	8 (1)	8.5
Sr	495 (1)	480	1 (1)	4.6
Y	12 (1)	12	5 (1)	1.8
Zr	309 (2)	300	4 (1)	11.7
Pb	32 (1)	29	3 (1)	2
Ba	1723 (45)	1850	n.d.	n.d.

av., sd and r.v. show average, standard deviation and recommended value, respectively.

5.b. Compositions of detrital material in bedded cherts

Concentrations of Al_2O_3, TiO_2, MgO, K_2O, and Zr in the samples show a clear inverse correlation in comparison to SiO_2 (correlation coefficients -0.97 to -0.99) (Table 3). This suggests that the bulk concentrations of these elements are diluted with radiolarian tests composed mostly of SiO_2 (e.g. Yamamoto, 1983). These elements are incorporated mainly in detrital material (including authigenic silicates), and therefore their mutual proportions can be indicators for the compositions of detrital material within the bedded cherts. In particular, Al, Ti and Zr are incorporated in solid phases in wide ranges of pH and Eh (e.g. Brookins, 1988), and therefore are thought to be immobile during diagenesis (e.g. Sugisaki, 1978; Sugisaki, Yamamoto & Adachi, 1982; Wintsch & Kvale, 1994; Yamamoto, Sugisaki & Arai, 1986). Their mutual proportions have often been used for estimating source-rock compositions of sediments and sedimentary rocks (Sugisaki, 1978; Sugitani, Sugisaki & Adachi, 1995; Garcia, Fonteilles & Moutte, 1994; Yamamoto, 1983).

The Al_2O_3/TiO_2 values in the bedded cherts show little variation (17–22; Fig. 5). The average values for the cherts and the shale-partings are 20.3 and 21.1, respectively. This implies that the detrital material supplied to the site of deposition had uniform values of

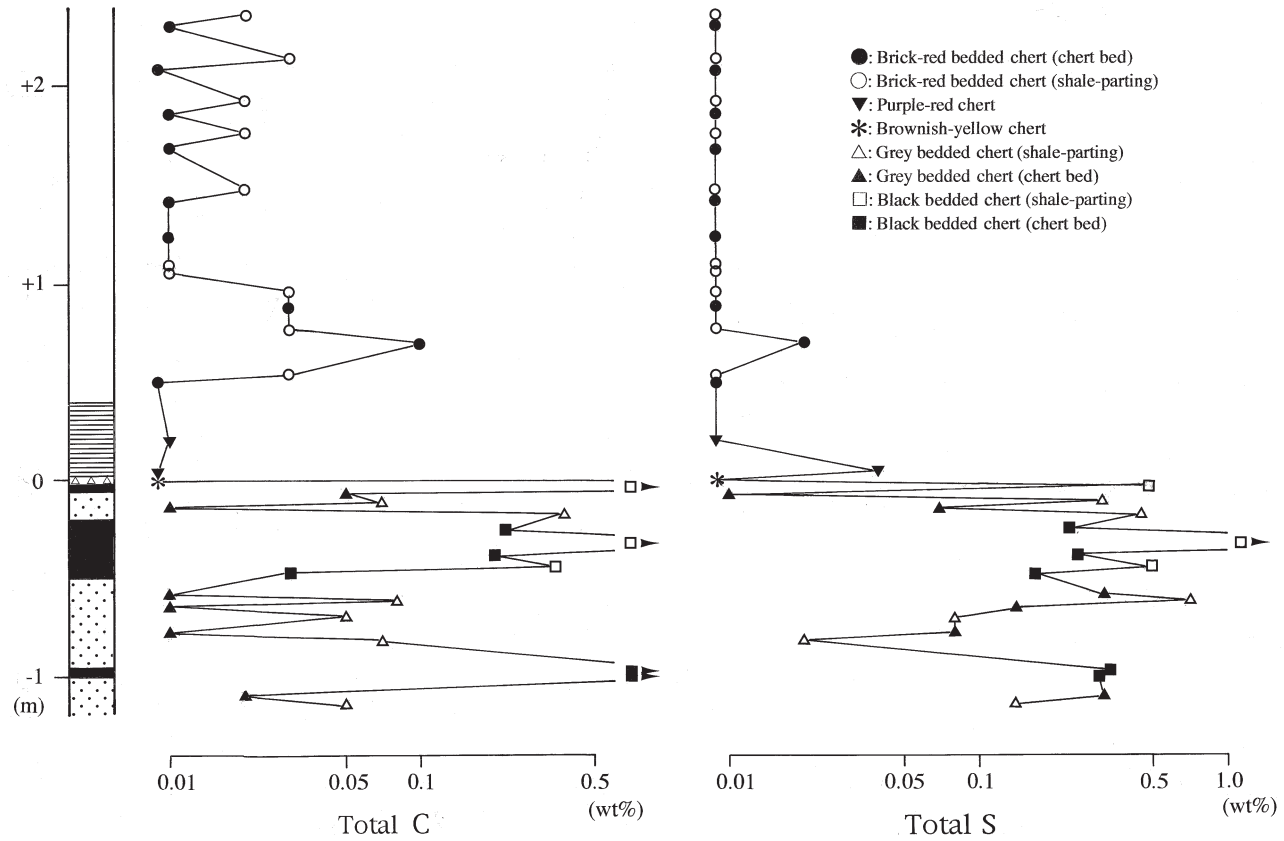

Figure 4. Stratigraphic variations for C_{tot} and S_{tot} concentrations. Open and closed symbols are for shale-partings (SiO_2 < 85%) and cherts (SiO_2 > 85%), respectively.

Table 3. Correlation coefficients for all samples

	SiO_2	TiO_2	Al_2O_3	MgO	K_2O	Zr
SiO_2	1.00	–0.99	–0.99	–0.97	–0.99	–0.99
TiO_2		1.00	0.99	0.97	0.99	0.99
Al_2O_3			1.00	0.98	0.99	0.99
MgO				1.00	0.98	0.96
K_2O					1.00	0.98
Zr						1.00

Al_2O_3/TiO_2. The values are consistent with previously reported Al_2O_3/TiO_2 values for Triassic bedded cherts in the Mino Belt (22.2 for cherts; Sugisaki, Yamamoto & Adachi, 1982; Yamamoto, 1983). Murray, Leinen & Isern (1993) and Murray & Leinen (1996) suggested that excess Al scavenged by organic compounds is present in marine biogenic sediments under high productivity zones. In addition, Murray, Jones & Buchholtz ten Brink (1992) showed that segregation between Al and Ti may occur during diagenesis of cherts. However, such effects as contribution of biogenic Al and diagenetic fractionation between Al and Ti cannot be seen in the bedded cherts in this study.

Zr/TiO_2 values tend to be uniform in the upper section, whereas they fluctuate slightly in the lower section (Fig. 5). Two samples in the lower section have remarkably high Zr/TiO_2 values compared to the other samples. Garcia, Fonteilles & Moutte (1994) showed that the Zr/TiO_2 value tends to be higher in sandstone than in shale of immature sedimentary suites due to hydraulic sorting between zircon ($ZrSiO_4$) and fine-grained rutile (TiO_2); fine-grained rutile is easily transported from source regions along with fine-grained aluminosilicates, whereas zircon tends to be less transported and is retained near source regions. Thus, higher Zr/TiO_2 values observed in the two samples could be attributed to the presence of coarse-grained detrital material such as zircon.

Values of K_2O/TiO_2 and MgO/TiO_2 in the bedded cherts show gradual increase from the lower to the upper part of the section (Fig. 5). Chemical fractionation of K_2O/TiO_2 between cherts and shales can also be seen.

It is interpreted that the detrital material in the bedded cherts was supplied from a common source throughout the deposition of the sequence, because Al_2O_3/TiO_2 and Zr/TiO_2 show little stratigraphic variation. Although the source rock compositions cannot be specified, the average values for Al_2O_3/TiO_2 (20.7) and Zr/TiO_2 (207) for all samples are similar to those

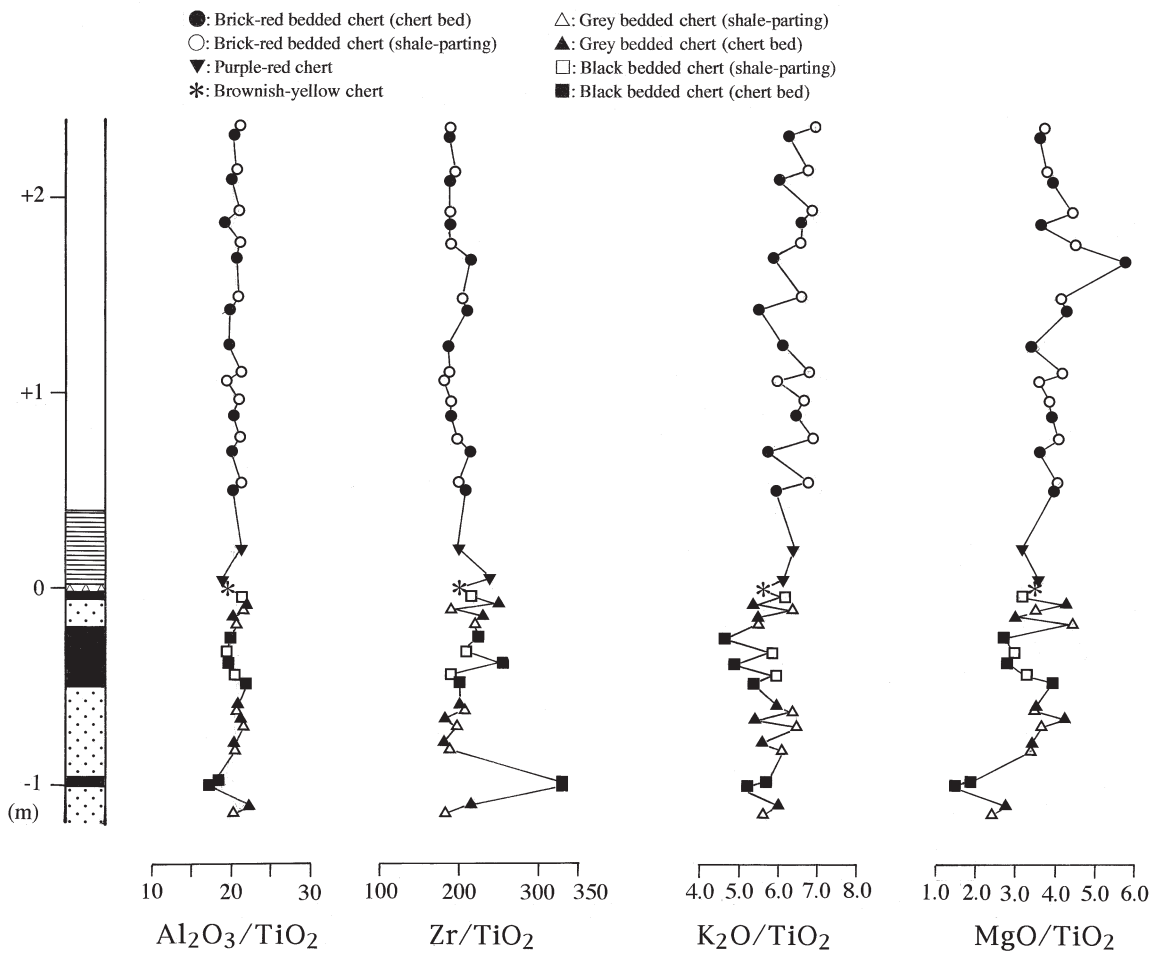

Figure 5. Stratigraphic variations for Al_2O_3/TiO_2, Zr/TiO_2, K_2O/TiO_2, and MgO/TiO_2.

of Meso-Cenozoic average greywacke (21.5 for Al_2O_3/TiO_2 and 201 for Zr/TiO_2), as recently estimated by Condie (1993). It can therefore be postulated that the composition of detrital material in the bedded cherts is equivalent to the Earth's upper crust. The homogeneity of detrital components throughout the bedded chert sequence would preclude the possibility that the stratigraphic geochemical variations were caused by the change in compositions of detrital material supplied to the site of deposition. Namely, geochemical variations observed in the bedded chert sequence can be explained mainly by other factors such as redox condition, microbial activities and formation of authigenic minerals. In the following discussions on geochemical characteristics of the bedded cherts, we use TiO_2-normalized values for some elements (Sugisaki, Yamamoto & Adachi, 1982; Sugisaki, 1984; Yamamoto, 1983), because bulk concentrations of constituent elements are diluted to various degrees by radiolarian-derived SiO_2. Hence, TiO_2 normalization can compensate the dilution of elemental concentrations by SiO_2 and enables us to compare the bedded cherts with less siliceous sediments and sedimentary rocks.

5.c. Major transition metals: Mn and Fe

The value of MnO/TiO_2 increases abruptly above the boundary (the brownish-yellow chert) between the upper and lower sections (Fig. 6). The average MnO/TiO_2 values (except for two outliers >0.7) are 0.26 (0.20–0.38) and 0.27 (0.15–0.49) for cherts and shales in the upper section, respectively, whereas in the lower section, they are 0.10 (0.03–0.18) and 0.08 (0.04–0.14), respectively. The two brick-red bedded cherts with high MnO/TiO_2 values (>0.7) tend to be enriched in C_{tot} concentrations compared with other brick-red bedded cherts. This implies that the authigenic carbonate grains in them (Fig. 3d) are Mn-bearing carbonates. The values of $Fe_2O_3^*/TiO_2$ ($Fe_2O_3^*$ = total Fe as Fe_2O_3) in the lower section tend to fluctuate more (6.0 to 13.1) than do those in the upper section samples (9.1 to 12.4, except one sample; Fig. 6). The value for the boundary sample (brownish-yellow

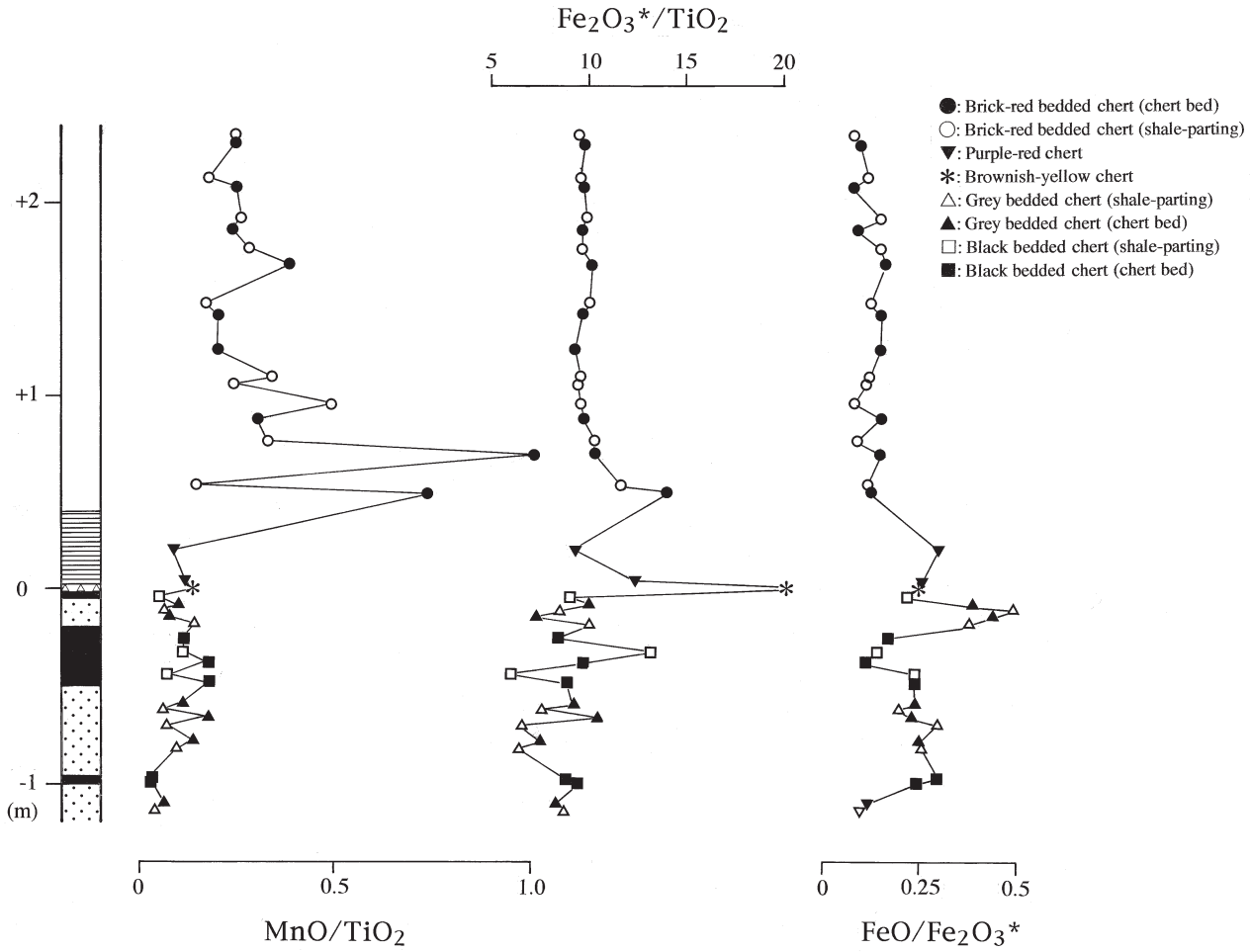

Figure 6. Stratigraphic variations for MnO/TiO_2, $Fe_2O_3^*/TiO_2$ and $FeO/Fe_2O_3^*$ ($Fe_2O_3^*$ = total Fe as Fe_2O_3). It should be noted that $FeO/Fe_2O_3^*$ values in the grey–black bedded cherts tend to be lower than their true values due to incomplete decomposition of pyrite by $HF–H_2SO_4$ (see text).

chert) is remarkably high (20.8). Values of FeO/Fe_2O_3* tend to be higher in the lower section than in the upper section.

5.d. Minor transition metals: Ni, Cu and Zn

Stratigraphic variations of TiO_2-normalized values of Ni, Cu and Zn show a similar trend (Fig. 7). The values in the lower section, if not all, tend to be higher than those in the upper section. Furthermore, within the lower section, TiO_2-normalized values of Ni and Zn in the cherts are remarkably fractionated from those in their adjacent shale-partings. The values in the upper section appear to be uniform in Figure 7. Values of Cu/TiO_2, on the other hand, are apparently higher in the cherts than their adjacent shale-partings throughout the sequence.

Enrichment factors relative to world-wide average shale $(= (element/Al)_{sample}/(element/Al)_{shale})$; Calvert & Pedersen, 1993) for the present bedded cherts (Fig. 8) tend to be larger than 1. The metal enrichment relative to the average shale is the most conspicuous in black bedded cherts, whose enrichment factors are mostly far larger than those for the modern organic-rich sediments from the Black Sea known to be enriched in some trace metals (Cu, Cd, Ni and Zn) due to sulphide precipitation (Calvert & Pedersen, 1993). Enrichment in several transition elements such as Cr, Cu, Mo, Ni, and Zn has been reported for other many carbonaceous and pyritic sediments and sedimentary rocks than the Black Sea sediments (Hatch & Leventhal, 1992; Calvert & Pedersen, 1993; Calvert, Bustin & Ingall, 1996). These elements are assumed to be present in syngenetic sulphides (Cu, Mo, Ni, and Zn) or are incorporated in kerogen (Mo and Ni) (e.g. Ripley, Shaffer & Gilstrap, 1990). Similar mechanisms are potentially responsible for metal enrichment in the black bedded cherts that contain abundant carbonaceous matter and pyrite.

5.e. Biogenic components: Ba, Sr and P

The values of Ba/TiO_2 and Sr/TiO_2 show conspicuous variation between cherts and shale-partings, and do not show an apparent stratigraphic trend (Fig. 9); the average values of Ba/TiO_2 and Sr/TiO_2 range from 760 to 1300 and from 170 to 340 in the cherts, respectively, and from 460 to 910 and from 60 to 110 in the shale-partings, respectively. The variation trend for P_2O_5/TiO_2 in the lower section bedded cherts is

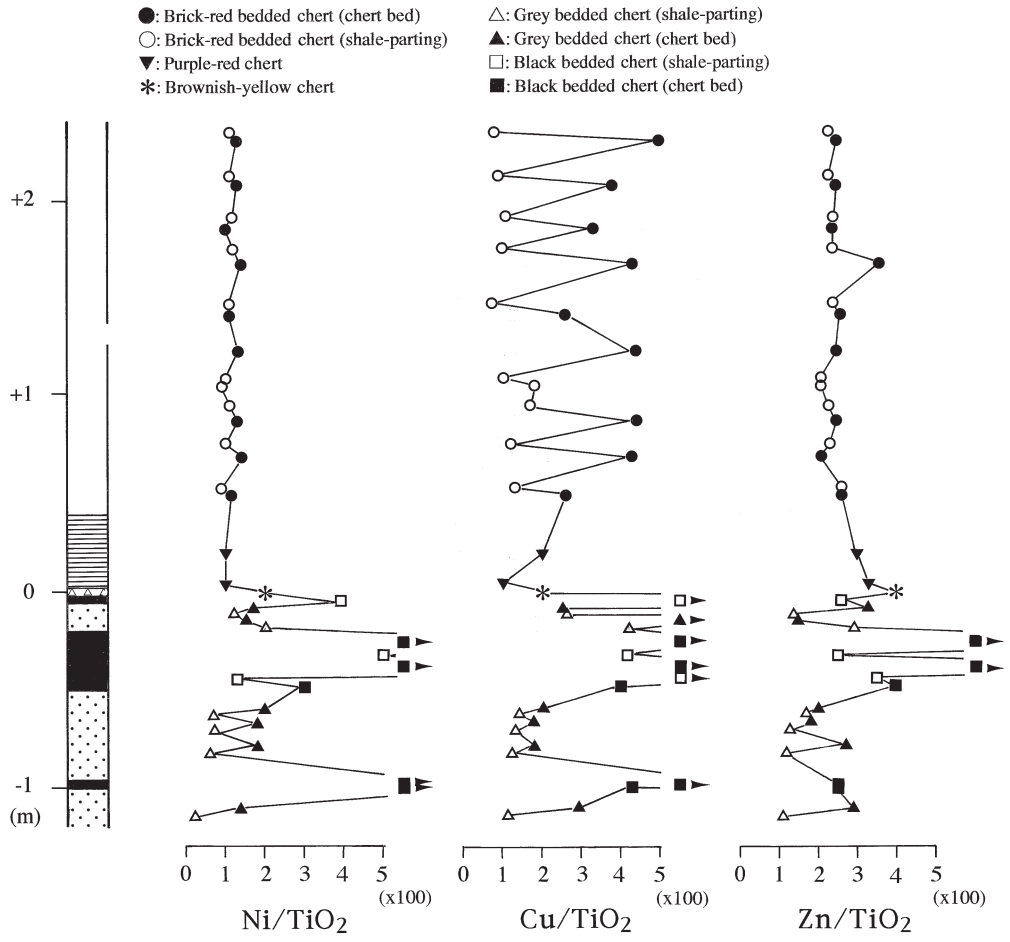

Figure 7. Stratigraphic variations for Ni/TiO_2, Cu/TiO_2 and Zn/TiO_2.

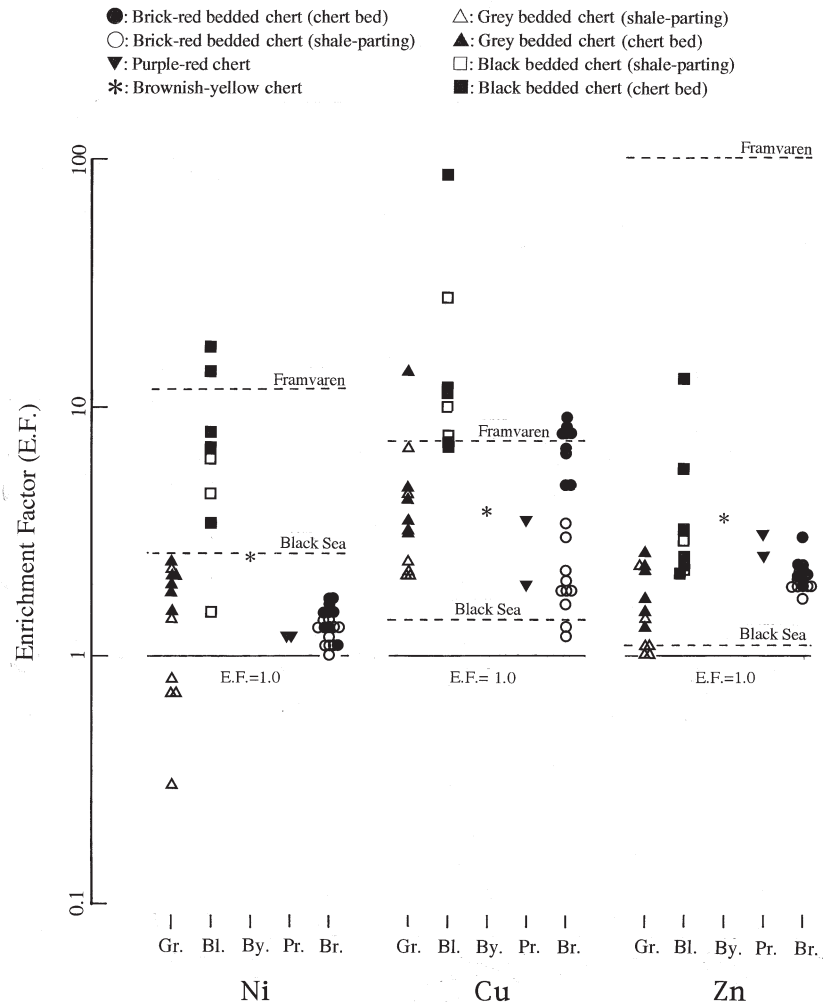

Figure 8. Enrichment factors for Ni, Cu and Zn. Enrichment factor is calculated as $(element/Al)_{sample}/(element/Al)_{shale}$ according to the definition of Calvert & Pedersen (1993). Horizontal dashed lines indicate enrichment factors for sediments from the Black Sea and Framvaren Fjord, modern anoxic basins; data for the Black Sea and Framvaren Fjord are quoted from Calvert & Pedersen (1993). Data for shale are quoted from Wedepohl (1971) according to Calvert & Pedersen (1993).

approximately similar to that for Ba/TiO_2 and Sr/TiO_2 (Fig. 9). In the upper section, however, the P_2O_5/TiO_2 value in shale-partings gradually increases and the uppermost four shale-partings have higher values than the adjacent cherts.

Barium is a biologically-mediated element in the ocean system and the mass flux of Ba to the ocean floor is primarily controlled by surface productivity (Schmitz, 1987; Dymond, Suess & Lyle, 1992). Sr-enriched barite, which is precipitated within remains of siliceous micro-organisms, may be a principal carrier of Ba and Sr (Dehairs, Stroobants & Goeyens, 1991; Dehairs, Chesselet & Jedwab, 1980; Bishop, 1988). The enrichment of Ba and Sr in cherts relative to shales for the present samples is analogically attributed to the presence of biogenic Sr-enriched barite in cherts that contain siliceous tests more than do adjacent shale-partings. Phosphorous is also regarded as an important tracer for palaeoproductivity of the ocean surface, but its variation trend in the present bedded cherts, especially in the upper section, does not synchronize with Ba and Sr; P_2O_5 concentrations of the cherts are not always higher than those of their adjacent shales. Positive correlation between P_2O_5 and CaO* (total Ca as CaO) (Fig. 10) implies that apatite is the most important sink for P in the bedded cherts. However, it should be noted that the positive correlation is largely derived from the uniform P_2O_5/CaO^* values in the upper section brick-red bedded cherts. Shale-partings of the lower section grey–black bedded cherts have higher P_2O_5/CaO^* values than the upper brick-red bedded cherts (Fig. 10). The complex stratigraphic variation trend of P could be attributed to diagenetic remobilization of P in sediments. Recent studies for diagenetic behavior of P in marine sediments suggest that P supplied to the ocean floor is mostly retained in sediments (Filippelli & Delaney, 1996), but reducing environments enhance regeneration and redistribution of P (Lucotte *et al.* 1994; Ingall & Jahnke, 1994; Ingall, Bustin & Van Cappellen,

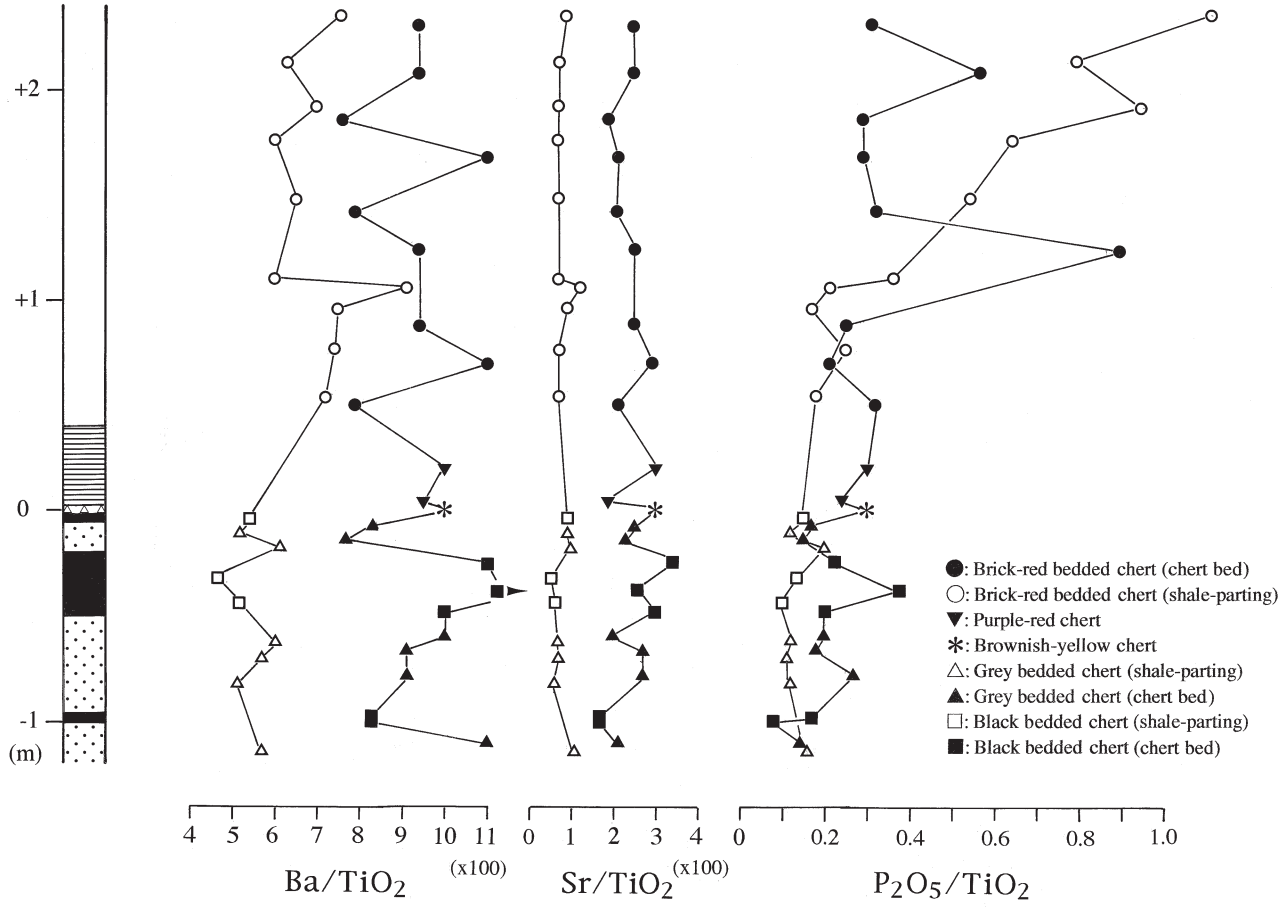

Figure 9. Stratigraphic variations for Ba/TiO_2, Sr/TiO_2 and P_2O_5/TiO_2.

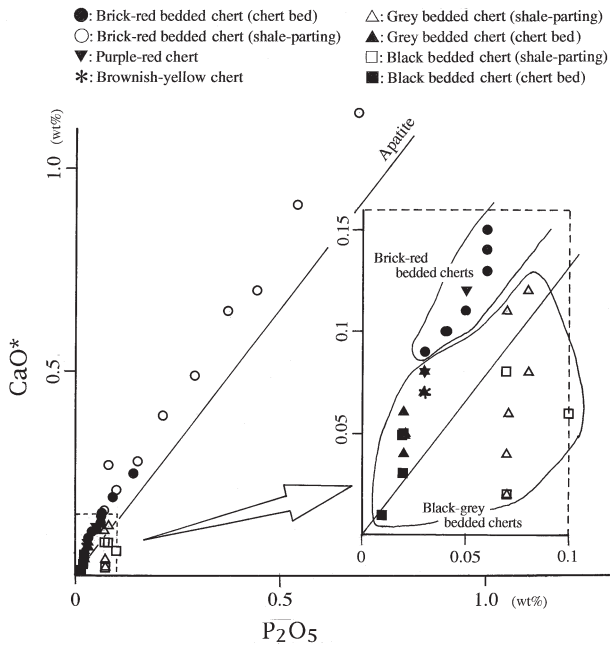

Figure 10. Relationships between concentrations of CaO* (total Ca as CaO) and P_2O_5.

1993). Additionally, the contribution of conodonts (composed of apatite) to bulk concentrations of P should have disturbed the trend of P linked to surface productivity. In fact, conodonts are often found in Triassic bedded cherts in the Mino Belt.

6. Synthesis and conclusions

6.a. The diagenetic environments of the bedded cherts

It is generally accepted that during the decomposition of organic matter in marine sediments, dissolved oxygen, Mn-oxides (MnO_2), nitrate, Fe-oxides (Fe_2O_3 and FeOOH), and sulphate are consumed in this order (Emerson *et al.* 1980; Froelich *et al.* 1979). If organic matter supplied to the sediments is completely decomposed before consumption of dissolved oxygen and Mn-oxides, anaerobic bacterial sulphate reduction (H_2S generation) and reduction of Fe^{3+} to Fe^{2+} would not occur (Curtis, 1987). Under this condition, framboidal pyrite formation, which requires high activities of coexisting dissolved Fe^{2+} and H_2S in porewaters,

does not occur. Hence, the presence of framboidal pyrite and carbonaceous matter in sediments indicates that the diagenetic environment for them had reached the stage of iron and sulphate reduction. In this context, stratigraphic variations of C_{tot}, S_{tot}, MnO/TiO_2, Fe_2O_3*/TiO_2, FeO/Fe_2O_3* and petrological features of the bedded cherts in this study can be concluded to record the change of sedimentary environments, which is summarized as follows by reference to the general scheme of diagenetic reactions.

During the deposition of the lower section, reactive Mn (Mn-oxides and -hydroxides) was completely reduced and subsequently reduction of Fe^{3+} (in oxides and silicates) and sulphate (in porewaters) occurred. The increase in activity of dissolved Fe^{2+} and H_2S in porewaters resulted in the formation of framboidal pyrite (Fig. 3b). Active dissolution and reprecipitation of Fe enhanced the redistribution and fractionation of Fe and other trace metals (Ni, Cu and Zn) between cherts and shale-partings (Figs 6 and 7). In contrast, the upper section bedded cherts were not subjected to early diagenetic sulphate reduction. Their MnO/TiO_2 values tend to be higher than the lower section samples (Fig. 6), suggesting that only a part of the reactive Mn-oxides were reduced. It can be assumed that organic matter supplied to the site of deposition was decomposed mostly by dissolved oxygen and partly by Mn-oxides or -nitrate during early diagenesis. The brick-red bedded chert samples with remarkably high MnO/TiO_2 values contain authigenic carbonates, which are assumed to be $MnCO_3$. These layers may be equivalents to Mn-carbonate bands (stratified Mn-carbonate deposits; Sugisaki, Sugitani & Adachi, 1991; Sugitani, 1989). It is well known that the stratified Mn-carbonate deposits are often associated with carbonaceous sediments (Force & Cannon, 1988; Huckriede & Meischner, 1996). The Mn-carbonate deposits are thought to have originated from surface oxidized Mn-rich layers that were derived from reprecipitation of dissolved Mn^{2+} migrating upward from underlying anoxic sediments (e.g. Sugisaki, Sugitani & Adachi, 1991; Sugitani, 1989). Calvert & Pedersen (1993) also emphasize that the presence of Mn-rich layers is a reliable indicator of bottom-water oxygenation.

The change of diagenetic processes described above is clearly identified by geochemical and mineralogical features of the boundary brownish-yellow chert. This chert abundantly contains goethite and is characterized by the highest Fe_2O_3*/TiO_2 values (Fig. 6). The goethite particles are possibly derived from oxidation of previously precipitated pyrite. The redox change from reducing to oxic conditions resulted in oxidation of previously-precipitated pyrite and the subsequent reprecipitation of Fe-hydroxides, which is likely to be responsible for Fe-enrichment relative to detrital components observed in this chert layer.

6.b. Geochemical constraints on sedimentary environments of the bedded cherts: pelagic or hemipelagic?

Sugisaki (1984) and Yamamoto (1983) discussed MnO/TiO_2 values in marine sediments of various depositional settings and showed that the value is a clue to sedimentary environments of fine-grained sedimentary rocks (bedded cherts and siliceous shales). In pelagic sediments under oxic conditions, Mn is retained in sediments as oxide or hydroxide, whereas in hemipelagic sediments under suboxic to anoxic conditions, Mn is dissolved as Mn^{2+} and migrates upward through the sedimentary column. Consequently, pelagic sediments are characterized by higher concentrations of Mn than hemipelagic sediments (Sugisaki, 1984; Yamamoto, 1983). This geochemical indicator is criticized by Murray (1994), who emphasizes that Mn-concentration is largely modified during diagenesis and that the concentration could not be a reliable indicator for sedimentary environments of ancient siliceous sediments such as cherts. Although Mn-redistribution between cherts and their shale-partings of bedded cherts certainly occurs in a particular case (e.g. Sugitani, 1996), the following lines of evidence indicate that the MnO/TiO_2 values in the bedded cherts studied here record sedimentary environments. In the bedded cherts, the stratigraphic variations of MnO/TiO_2 values in cherts and their shale-partings are synchronized with each other and the stratigraphic trend of MnO/TiO_2 is consistent with the change of sedimentary environments deduced from other geochemical characteristics (C_{tot} and S_{tot}, FeO/Fe_2O_3*) and petrological features (abundant carbonaceous matter and framboidal pyrite in the lower section). Accordingly, at least in the present case, the MnO/TiO_2 value can be concluded to be a reliable indicator of sedimentary environments.

The upper section brick-red bedded cherts have higher MnO/TiO_2 values than do the lower ones, indicating more oxidizing environments as discussed in Section 6.a. Their values (average 0.26 for cherts except two samples and average 0.27 for shale-partings), however, are still lower than those for pelagic sediments in central Pacific regions ($MnO/TiO_2 > 1$; Sugisaki, Yamamoto & Adachi, 1982; Yamamoto, 1983; Sugisaki, 1984). This suggests that the bedded cherts were deposited in hemipelagic regions. The result is consistent with those of previous studies for bedded cherts in the Mino Belt (Yamamoto, 1983; Sugisaki, Yamamoto & Adachi, 1982; Matsumoto & Iijima, 1983; Sugitani, 1989; Shimizu & Masuda, 1977). Contribution of hydrothermal components (Fe, Mn and Si) is excluded by the Fe_2O_3*/TiO_2–$Al_2O_3/(Al_2O_3 + Fe_2O_3*)$ plot (Murray, 1994) (Fig. 11), where the bedded cherts are distributed within the area for both pelagic sediments and continental margin ones. This plot indicates that the present samples were formed far from ridges and

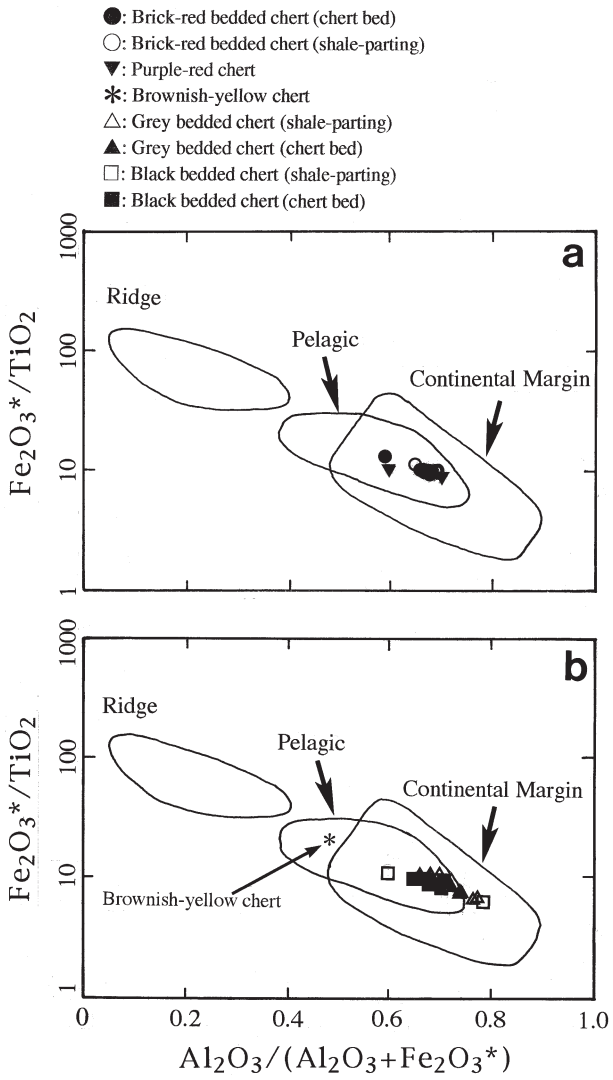

Figure 11. Relationships between Fe_2O_3*/TiO_2 and $Al_2O_3/(+Al_2O_3Fe_2O_3*)$ (Murray, 1994): (a) for brick-red bedded cherts; (b) for black bedded cherts, grey bedded cherts and brownish-yellow chert.

were not influenced by hydrothermal activities. This is not inconsistent with the fact that basaltic rocks are not found around the bedded chert sequence in this study.

6.c. Critical re-examination of the 'superanoxia' model for the formation of carbonaceous bedded cherts

Nakao & Isozaki (1994) and Kubo, Isozaki & Matsuo (1996) suggested that the carbonaceous grey–black bedded cherts in the Mino Belt were deposited under euxinic environments developed in the world ocean (superanoxia; Isozaki, 1997). On the basis of the pelagic origin of bedded cherts in the Mino Belt, these authors claimed that the 'superanoxia' started from the end-Permian regression and continued until the Middle Triassic; seawater stratification resulting from the world-wide regression and the development of anoxic deep water facilitated the deposition of carbonaceous cherts. We also suggest that the sea-level regression and resultant development of anoxic sedimentary environment were responsible for the formation of carbonaceous bedded cherts. However, it must be emphasized that the 'superanoxia' model proposed by Isozaki (1997) is not a unique explanation for the formation of carbonaceous bedded cherts, because the end-Permian sea-level regression had already been recovered in Early Triassic time (Embry, 1988) and the site of deposition for the Triassic bedded cherts in the Mino Belt is still controversial. Thus, the current interpretation of Triassic bedded cherts in the Mino Belt as pelagic sediments (e.g. Matsuda & Isozaki, 1991) and the 'superanoxia' model (Isozaki, 1997) for the formation of carbonaceous bedded cherts should be re-examined carefully.

If the end-Permian sea-level regression had already been recovered in Early Triassic time (Embry, 1988), it is unlikely that the world-wide sea-water stratification had continued for nearly 20 m.y. from end-Permian to Middle Triassic time (Isozaki, 1997). Embry (1988) also showed that several cycles of sea-level change had occurred during the Triassic. The sea-level regression potentially responsible for water column anoxia and the deposition of carbonaceous cherts may correspond to that which occurred in the Triassic rather than at the end of the Permian. As shown by Kubo, Isozaki & Matsuo (1996), a few cycles of grey–black bedded cherts and brick-red bedded cherts are recognized within the Early to Middle Triassic bedded chert sequence in the Mino Belt, implying that an oxic sedimentary environment suggested by the deposition of brick-red bedded cherts had been developed before the deposition of the grey–black bedded cherts under discussion herein. A brick-red bedded chert unit, though not observed at our sampling site, may be present below the lower section grey–black bedded cherts.

Although bedded cherts containing abundant radiolarian remains and lacking coarse detrital material in the Mino Belt are generally believed to have been deposited in pelagic regions (below the carbonate compensation depth) far from land and accreted at ancient subduction zones (e.g. Matsuda & Isozaki, 1991), the site of deposition of bedded cherts is not necessarily deep and pelagic. Radiolarites in the Tethyan region, for example, are thought to have been deposited in shallow environments with estimated depths of 1500 to 2000 m at continental margins (De Wever *et al.* 1995; Iijima *et al.* 1978). Absence of coarse detrital material in bedded cherts can also be explained by deposition on banks or in basins protected from detrital input by swells. It should be also emphasized that the results of most geochemical studies of bedded cherts, including ours, are not inconsistent with the semi-closed marginal basin model for the Mino Belt proposed firstly by Adachi (1976) and recently provided with new geochronological evidence of detrital monazite (Suzuki, Adachi & Tanaka, 1991).

6.d. Alternative model for the formation of carbonaceous bedded cherts and implications for origins of organic matter

It is well known that in closed or semi-closed oceanic basins such as the Black Sea and the Sea of Japan, redox change of the sedimentary environment was caused by sea-level change. In the Black Sea, a well-aerated fresh-water environment was shifted to a reducing marine environment from 7000 years B.P., due to sea-level rise and inflow of Mediterranean sea-water. Development of density stratification of the basin water resulted in an anoxic environment in the bottom waters and sedimentation of organic-rich layers (Ross & Degens, 1974). Conversely, the sedimentation of most, if not all, Quaternary organic- and/or sulphur-rich dark layers in the Sea of Japan has been caused by sea-level falls; during regressions, the Sea of Japan was isolated from open oceans and the circulation and renewal of the basin water were restricted, resulting in the development of anoxic sedimentary environments (e.g., Masuzawa & Kitano, 1984; Nakajima *et al.* 1996). In both cases, the closed or semi-closed setting enhances the fluctuation of sedimentary environments of ocean basins due to sea-level changes. Analogically, the deposition of carbonaceous bedded cherts examined here can also be interpreted by the sea-level regression and subsequent development of anoxic sedimentary environment that had occurred in a marginal and semi-closed basin in the Triassic. Namely, during Triassic sea-level regressions (Embry, 1988), the site of deposition of the Mino Belt was at least partially isolated from the open ocean, resulting in the restricted circulation and renewal of basin water. Restricted basin-water circulation and renewal probably kept dissolved oxygen in the basin water at a low level, enhancing the preservation of organic matter and the formation of carbonaceous cherts.

In the above discussions, we have emphasized low dissolved oxygen in the water column (water-column anoxia) as a major cause for the deposition of carbonaceous bedded cherts. However, factors controlling the preservation of organic matter in marine sediments include high sedimentation rate and high productivity in surface water other than water-column anoxia (Canfield, 1994). Organic-rich sediments are also formed in the intermediate-depth oxygen minimum zone and upwelling zone on continental margins, plataeux and so on (e.g. Thiede & van Andel, 1977). Sedimentation rate and/or surface productivity do not appear to have been drastically higher during the period of deposition of carbonaceous cherts, because the compositions of detrital components are uniform, and both the lower and upper section bedded cherts commonly contain abundant radiolarian tests. These facts could preclude the possibility that high sedimentation rate and high surface productivity were responsible for the deposition of carbonaceous cherts, but further investigations including analyses of carbon and sulphur isotopes would be required in order to specify the major factor controlling the preservation of organic matter. Additionally, the origin of organic matter preserved in the carbonaceous cherts is another problem to be resolved. Carbonaceous matter preserved in the bedded cherts has two potential origins; settling organic particles of radiolaria and phytoplankton from the surface water, and remains of bacteria propagated within sediments. Since the biologically-mediated active sulphate reduction occurred during the sedimentation of carbonaceous grey–black bedded cherts, organic matter in them was derived at least partially from remains of sulphate-reducing bacteria (e.g. some species of *Desulfovibrio*). Also, organic mats formed by sulphur bacteria such as *Thioploca* and *Begiatoa* (Gallardo, 1977; Sweerts *et al.* 1990) may also have been precursors of carbonaceous matter. Mats of *Thioploca* were recovered from continental shelf underlain by a low dissolved-O_2 upwelling water mass off Peru and Chile (Gallardo, 1977). Fossing *et al.* (1995) show that *Thioploca*, depending on coexisting electron donors (H_2S) and electron acceptors (O_2 or NO_3^-), can thrive within NO_3^--deficient reducing sediments by the mechanism of NO_3^- transportation and concentration from the overlying sea-water. Abundant framboidal pyrite in the carbonaceous bedded cherts in the Mino Belt indicates high concentration of H_2S in sediments, which could not preclude the possibility of propagation of mat-forming sulphur bacteria as well as sulphate-reducing bacteria during the sedimentation of the carbonaceous cherts.

7. Summary

The present study reveals an abrupt change of sedimentary environments of Triassic bedded cherts in the Mino Belt, central Japan. The change of diagenetic environments from anoxic to suboxic is imprinted on their geochemical and mineralogical characteristics in the chert sequence. On the basis of the results obtained by this study, we summarize the palaeoceanography and sedimentary systems of Triassic bedded cherts, as follows.

(1) The studied bedded chert sequence is subdivided into the lower grey–black bedded cherts and the upper brick-red bedded cherts. The brownish-yellow and purple-red cherts are present at the boundary between both types. The grey–black bedded cherts are enriched in carbonaceous matter and framboidal pyrite, whereas the brick-red bedded cherts do not contain them. Hematite is present in the brick-red bedded cherts and the purple-red bedded chert, but not in the grey–black bedded cherts.

(2) The differences in mineral assemblages between the lower section bedded cherts and the upper section bedded cherts are consistent with the stratigraphic variations of some geochemical signatures such as MnO/TiO_2, $Fe_2O_3{*}/TiO_2$, $FeO/Fe_2O_3{*}$, C_{tot} and S_{tot}.

(3) The diagenetic environment of the lower section bedded cherts was apparently more reducing than that of the upper section bedded cherts; the lower section bedded cherts were subjected to early diagenetic sulphate reduction, whereas the upper section ones were not.

(4) The formation of carbonaceous and pyritic bedded cherts may have been caused by the sea-level regression that occurred during the Triassic. During the sea-level regression, the site of deposition might have been isolated from the open ocean, and the circulation and renewal of the basin water were restricted, resulting in the development of a reducing sedimentary environment and diagenetic process.

Acknowledgements. We thank the members of the Department of Natural Science Informatics and the Department of Earth and Planetary Sciences of Nagoya University. We wish to express our gratitude to Dr K. Suzuki, Dr K. Yamamoto and Dr M. Ito, who advised us on XRF analyses of major elements; to Mr S. Yogo and Mr T. Nagaoka, who prepared thin sections for the samples; to Dr T. Matsubara, who advised us on mat-forming sulphur bacteria. We are also indebted to Dr H. Maekawa in Kobe University for XRF analyses of minor elements, and to Dr R. Sugisaki in Meijyo University for his helpful comments on our manuscript.

References

Adachi, M. 1976. Paleogeographic aspects of the Japanese Paleozoic-Mesozoic geosyncline. *The Journal of Earth Sciences, Nagoya University* **23/24**, 13–55.

Adachi, M., Yamamoto, K. & Sugisaki, R. 1986. Hydrothermal chert and associated siliceous rocks from the northern Pacific: Their geological significance as indication of ocean ridge activity. S*edimentary Geology* **47**, 125–48.

Berner, R. A. 1984. Sedimentary pyrite formation: An update. *Geochimica et Cosmochimica Acta* **48**, 605–15.

Bishop, J. K. B., 1988. The barite–opal–organic carbon association in oceanic particulate matter. *Nature* **332**, 341–3.

Boström, K. Kraemer, T. & Gartner, S. 1973. Provenance and accumulation rates of opaline silica, Al, Ti, Fe, Mn, Cu, Ni and Co in Pacific pelagic sediments. *Chemical Geology* **11**, 123–48.

Brookins, D. G. 1988. *Eh–pH Diagrams for Geochemistry*. Berlin: Springer-Verlag.

Calvert, S. E., Bustin, R. M. & Ingall, E. D. 1996. Influence of water column anoxia and sediment supply on the burial and preservation of organic carbon in marine shales. *Geochimica et Cosmochimica Acta* **60**, 1577–93.

Calvert, S. E. & Pedersen, T. F. 1993. Geochemistry of Recent oxic and anoxic marine sediments: Implications for the geological record. *Marine Geology* **113**, 67–88.

Canfield, D. E. 1994. Factors influencing organic carbon preservation in marine sediments. *Chemical Geology* **114**, 315–29.

Cluzel, D. 1991. Late Palaeozoic to early Mesozoic geodynamic evolution of the Circum-Pacific orogenic belt in South Korea and Southwest Japan. *Earth and Planetary Science Letters* **108**, 289–305.

Condie, K. C. 1993. Chemical composition and evolution of the upper continental crust: Contrasting results from surface samples and shales. *Chemical Geology* **104**, 1–37.

Curtis, C. D. 1987. Mineralogical consequences of organic matter degradation in sediments: inorganic/organic diagenesis. In *Marine Clastic Sedimentology* (eds J. K. Leggett and G. G. Zuffa), pp. 108–23. London: Graham & Trotman.

Dehairs, F., Chesselet, R. & Jedwab, J. 1980. Discrete suspended particles of barite and the barium cycle in the open ocean. *Earth and Planetary Science Letters* **49**, 528–50.

Dehairs, F., Stroobants, N. & Goeyens, L. 1991. Suspended barite as a tracer of biological activity in the Southern Ocean. *Marine Chemistry* **35**, 399–410.

De Wever, P., Baudin, F., Azéma, J. & Fourcade, E. 1995. Radiolarians and Tethyan radiolarites from primary production to their paleogeography. In *The Ocean Basins and Margins. Volume 8: The Tethys Ocean* (eds A. E. M. Nairn *et al*.), pp. 267–318. New York, London: Plenum Press.

Dymond, J., Suess, E. & Lyle, M. 1992. Barium in deep-sea sediment: A geochemical proxy for paleoproductivity. *Paleoceanography* **7**, 163–81.

Embry, A. F. 1988. Triassic sea-level changes: evidence from the Canadian Arctic Archipelago. In *Sea-level changes: an integrated approach* (eds C. K. Wilgus *et al*.), pp. 249–59. Society of Economic Paleontologists and Mineralogists, Special Publication no. 42.

Emerson, S., Jahnke, R., Bender, M., Froelich, P., Klinkhammer, G., Bowser, C. & Setlock, G. 1980. Early diagenesis in sediments from the eastern equatorial Pacific, I. Pore water nutrient and carbonate results. *Earth and Planetary Science Letters* **49**, 57–80.

Filippelli, , G. M. & Delaney, M. L. 1996. Phosphorus geochemistry of equatorial Pacific sediments. *Geochimica et Cosmochimica Acta* **60**, 1479–95.

Force, E. R. & Cannon, W. F. 1988. Depositional model for shallow-marine manganese deposits around black shale basins. *Economic Geology* **83**, 93–117.

Fossing, H., Gallardo, V. A., Jørgensen, B. B., Hüttel, M., Nielsen, L. P., Schulz, H., Canfield, D. E., Forster, S., Glud, R. N., Gundersen, J. K., Küver, J., Ramsing, N. B., Teske, A., Thamdrup, B. & Ulloa, O. 1995. Concentration and transport of nitrate by the mat-forming sulphur bacterium *Thioploca*. *Nature* **374**, 713–15.

Froelich, P. N., Klinkhammer, G. P., Bender, M. L., Luedtke, N. A., Heath, G. R., Cullen, D., Dauphin, P., Hammond, D., Hartman, B. & Maynard, V. 1979. Early oxidation of organic matter in pelagic sediments of the eastern equatorial Atlantic: suboxic diagenesis. *Geochimica et Cosmochimica Acta* **43**, 1075–90.

Garcia, D., Fonteilles, M. & Moutte, J. 1994. Sedimentary fractionations between Al, Ti, and Zr and the genesis of strongly peraluminous granites. *Journal of Geology* **102**, 411–22.

Gallardo, V. A. 1977. Large benthic microbial communities in sulphide biota under Peru-Chile Subsurface Countercurrent. *Nature* **268**, 331–2.

Geological Survey of Japan. 1992. *1 : 200 000 Geological Map, Gifu.*

Girty, G. H., Ridge, D. L., Knaack, C., Johnson, D. & Al-Riyami, R. K. 1996. Provenance and depositional setting of Paleozoic chert and argillite, Sierra Nevada, California. *Journal of Sedimentary Research* **66**, 107–18.

HATCH, J. R. & LEVENTHAL, J. S. 1992. Relationship between inferred redox potential of the depositional environment and geochemistry of the Upper Pennsylvanian (Missourian) Stark Shale Member of the Dennis Limestone, Wabaunsee County, Kansas, U.S.A. *Chemical Geology* **99**, 65–82.

HUCKRIEDE, H. & MEISCHNER, D. 1996. Origin and environment of manganese-rich sediments within black-shale basins. *Geochimica et Cosmochimica Acta* **60**, 1399–413.

IIJIMA, A., KAKUWA, Y., YAMAZAKI, K. & YANAGIMOTO, Y. 1978. Shallow-sea, organic origin of the Triassic bedded chert in central Japan. *Journal of the Faculty of Science, the University of Tokyo, Section II* **19**, 369–400.

INGALL, E. D., BUSTIN, R. M. & VAN CAPPELLEN, P. 1993. Influence of water column anoxia on the burial and preservation of carbon and phosphorous in marine shales. *Geochimica et Cosmochimica Acta* **57**, 303–16.

INGALL, E. & JAHNKE, R. 1994. Evidence for enhanced phosphorus regeneration from marine sediments overlain by oxygen depleted waters. *Geochimica et Cosmochimica Acta* **58**, 2571–5.

ISOZAKI, Y. 1997. Permo-Triassic boundary superanoxia and stratified superocean: records from lost deep sea. *Science* **276**, 235–8.

KNAUTH, L. P. 1994. Petrogenesis of cherts. In *Silica: Physical Behavior, Geochemistry and Materials Applicaions* (eds P. J. Hearley, C. T. Prewitt and G. V. Gibbs), pp. 233–58. Mineralogical Society of America Reviews in Mineralogy no. 29.

KUBO, K., ISOZAKI, Y. & MATSUO, M. 1996. Color of bedded chert and redox condition of depositional environment: ^{57}Fe Mössbauer spectroscopic study on chemical state of iron in Triassic deep-sea pelagic chert. *Journal of Geological Society of Japan* **102**, 40–8.

LUCOTTE, M., MUCCI, A., HILLAIRE-MARCEL, C. & TRAN, S. 1994. Early diagenetic processes in deep Labrador Sea sediments: reactive and nonreactive iron and phosphorous. *Canadian Journal of Earth Sciences* **31**, 14–27.

MARUYAMA, S. & SENO, T. 1986. Orogeny and relative plate motions: example of the Japanese Islands. *Tectonophysics* **127**, 305–29.

MASUZAWA, T. & KITANO, Y. 1984. Appearance of H_2S-bearing bottom waters during the last glacial period in the Japan Sea. *Geochemical Journal* **18**, 167–72.

MATSUMOTO, R. & IIJIMA, A. 1983. Chemical sedimentology of some Permo-Jurassic and Tertiary bedded cherts in central Honshu, Japan. In *Siliceous Deposits in the Pacific Region* (eds A. Iijima, J. R. Hein and R. Siever), pp. 175–91. Amsterdam, Oxford, New York: Elsevier.

MATSUDA, T. & ISOZAKI, Y. 1991. Well-documented travel history of Mesozoic pelagic chert in Japan: from remote ocean to subduction zone. *Tectonics* **10**, 475–99.

MIZUTANI, S. 1987. Mesozoic Terranes in the Japanese Islands and neighbouring East Asia. *Geodynamics Series* **19**, 263–73.

MURRAY, R. W. 1994. Chemical criteria to identify the depositional environment of chert: general principles and applications. *Sedimentary Geology* **90**, 213–32.

MURRAY, R. W., BUCHHOLTZ TEN BRINK, M. R., GERLACH, D. C., RUSS, G. P. III & JONES, D. L. 1991. Rare earth, major and trace elements in chert from the Franciscan Complex and Monterey Group, California: Assessing REE sources to fine-grained marine sediments. *Geochimica et Cosmochimica Acta* **55**, 1875–95.

MURRAY, R. W., JONES, D. L. & BUCHHOLTZ TEN BRINK, M. R. 1992. Diagenetic formation of bedded chert: Evidence from chemistry of the chert-shale couplet. *Geology* **20**, 271–4.

MURRAY, R. W. & LEINEN, M. 1996. Scavenged excess aluminum and its relationship to bulk titanium in biogenic sediment from the central equatorial Pacific Ocean. *Geochimica et Cosmochimica Acta* **60**, 3869–78.

MURRAY, R. W., LEINEN, M. & ISERN, A. R. 1993. Biogenic flux of Al to sediment in the Central Equatorial Pacific Ocean; evidence for increased productivity during glacial episodes. *Paleoceanography* **8**, 651–70.

NAKAJIMA, T., KIKKAWA, K., IKEHARA, K., KATAYAMA, H., KIKAWA, E., JOSHIMA, M. & SETO, K. 1996. Marine sediments and late Quaternary stratigraphy in the southeastern part of the Japan Sea – Concerning the timing of dark layer deposition. *Journal of Geological Society of Japan* **102**, 125–38.

NAKAO, K. & ISOZAKI, Y. 1994. Recovery history from the P/T boundary deep-sea anoxia recorded in pelagic chert in the Inuyama area, Mino Belt, Southwest Japan. *Journal of Geological Society of Japan* **100**, 505–8.

NISBET, E. G. & PRICE, I. 1974. Siliceous turbidite: bedded cherts as redeposited, ocean ridge-derived sediments. In *Pelagic Sediments: on Land and under the Sea* (eds K. J. Hsü and H. C. Jenkyns), pp. 351–66. International Association of Sedimentologists, Special Publication no. 1. Oxford: Blackwell.

RIPLEY, E. M., SHAFFER, N. R. & GILSTRAP, M. S. 1990. Distribution and geochemical characteristics of metal enrichment in the New Albany Shale (Devonian–Mississippian), Indiana. *Economic Geology* **85**, 1790–807.

ROSS, D. A. & DEGENS, E. T. 1974. Recent sediments of the Black Sea. In *The Black Sea – Geology, Chemistry, and Biology* (eds E. T. Degens and D. A. Ross), pp. 183–99. American Association of Petroligists and Geologists Memoir no. 20.

SCHMITZ, B. 1987. Barium, equatorial high productivity, and the northward wandering of the Indian continent. *Paleoceanography* **2**, 63–77.

SHIMIZU, H. & MASUDA, A. 1977. Cerium in chert as an indication of marine environment of its formation. *Nature* **266**, 346–8.

STEINBERG, M., BONNOT-COURTIS, C. & TLIG, S. 1983. Geochemical contribution to the understanding of bedded chert. In *Siliceous Deposits in the Pacific Region* (eds A. Iijima, J. R. Hein and R. Siever), pp. 193–210. Amsterdam, Oxford, New York: Elsevier.

SUGISAKI, R. 1978. Chemical composition of argillaceous sediments on the Pacific margin of Southwest Japan. In *Investigations of the continental margin of Southwest Japan* (ed. E. Inoue), pp. 65–73. Geological Survey of Japan Cruise Report no. 9.

SUGISAKI, R. 1981. A modified method of analysis of bulk chemical composition of argillaceous sediments and data display with special reference to marine sediments. *Journal of Geological Society of Japan* **87**, 77–85.

SUGISAKI, R. 1984. Relation between chemical composition and sedimentation rate of Pacific ocean-floor sediments deposited since the Middle Cretaceous: Basic evidence for chemical constraints on depositional environments of ancient sediments. *Journal of Geology* **92**, 235–59.

SUGISAKI, R., SUGITANI, K. & ADACHI, M. 1991. Manganese carbonate bands as an indicator of hemipelagic sedimentary environments. *Journal of Geology* **99**, 23–40.

SUGISAKI, R., SHIMOMURA, T. & ANDO, K. 1977. An automatic X-ray fluorescence method for the analysis of sili-

cate rocks. *Journal of Geological Society of Japan* **83**, 725–33.

Sugisaki, R., Yamamoto, K. & Adachi, M. 1982. Triassic bedded cherts in central Japan are not pelagic. *Nature* **298**, 644–7.

Sugitani, K. 1989. Geochemistry of manganese bands hosted by sedimentary rocks in the Mino Terrane, central Japan: Its comparison with marine sediments and the geological significance. *Journal of Geological Society of Japan* **95**, 255–75.

Sugitani, K. 1996. Study of sedimentary paleoenvironments of siliceous sedimentary rocks using some geochemical indicators. *Chikyukagaku (Geochemistry)* **30**, 75–89.

Sugitani, K., Sano, H., Adachi, M. & Sugisaki, R. 1991. Permian hydrothermal deposits in the Mino Terrane, central Japan; implications for hydrothermal plumes in an ancient ocean basin. *Sedimentary Geology* **71**, 59–71.

Sugitani, K., Sugisaki, R. & Adachi, M. 1995. Authigenic carbonate concretions and host shales from the Shimanto Belt, southwestern Japan: Implications for carbonate precipitation. *Journal of Sedimentary Research* **A65**, 531–40.

Sugiyama, K. 1995. Triassic radiolarian biostratigraphy in the southeastern part of the Mino Terrane. *Abstracts of the 1995 annual meeting of the Palaeontological Society of Japan*, p. 124.

Suzuki, K., Adachi, M. & Tanaka, T. 1991. Middle Precambrian provenance of Jurassic sandstone in the Mino Terrane, central Japan: Th–U–total Pb evidence from an electron microprobe monazite study. *Sedimentary Geology* **75**, 141–7.

Sweerts, J.-P. R. A., De Beer, D., Nielsen, L. P., Verdouw, H., Van den Heuvel, J. C., Cohen, Y. & Cappenberg, T. E. 1990. Denitrification by sulphur oxidizing *Beggiatoa* spp. mats on freshwater sediments. *Natur*e **344**, 762–3.

Taira, A., Pickering, K. T., Windley, B. F. & Soh, W. 1992. Accretion of Japanese Island Arcs and implications for the origin of Archean greenstone belts. *Tectonics* **11**, 1224–44.

Thiede, J. & van Andel, T. H. 1977. The paloenvironment of anaerobic sediments in the late Mesozoic South Atlantic Ocean. *Earth and Planetary Science Letters* **33**, 301–9.

Wakita, K.1988. Origin of chaotically mixed rock bodies in the Early Jurassic to Early Cretaceous sedimentary complex of the Mino Terrane, central Japan. *Bulletin of the Geological Survey of Japan* **39**, 675–757.

Wedepohl, K. H. 1971. Environmental influences on the chemical composition of shales and clays. In *Physics and Chemistry of the Earth, Volume 8* (eds L. H. Ahrens, F. Press, S. K. Runcorn and H. C. Urey), pp. 307–31. Oxford: Pergamon.

Wintsch, R. P. & Kvale, C. M. 1994. Differential mobility of elements in burial diagenesis of siliciclastic rocks. *Journal of Sedimentary Research* **A64**, 349–61.

Yamamoto, K. 1983. Geochemical study of Triassic bedded cherts from Kamiaso, Gifu Prefecture. *Journal of Geological Society of Japan* **89**, 143–62.

Yamamoto, K. 1984. Geochemical study of acidic tuffs and siliceous shales from the Setogawa Terrane in the western part of Shizuoka City. *Journal of Geological Society of Japan* **90**, 479–96.

Yamamoto, K. 1987. Geochemical characteristics and depositional environments of cherts and associated rocks in the Franciscan and Shimanto Terranes. *Sedimentary Geology* **52**, 65–108.

Yamamoto, K., Sugisaki, R. & Arai, F. 1986. Chemical aspects of alteration of acidic tuffs and their application to siliceous deposits. *Chemical Geology* **55**, 61–76.

Yao, A., Matsuda, T. & Isozaki, Y. 1980. Triassic and Jurassic radiolarians from the Inuyama area, central Japan. *Journal of Geoscience, Osaka City University* **23**, 135–54.